PERGAMON

Journal of Structural Geology 24 (2002) 1109–1123

JOURNAL OF STRUCTURAL GEOLOGY

www.elsevier.com/locate/jstrugeo

A comparison of microstructural and chemical patterns in garnet from the Fleur de Lys Supergroup, Newfoundland

Aaron Stallard*, Ken Hickey[1]

School of Earth Sciences, James Cook University, Townsville 4811, Australia

Received 25 January 2001; revised 1 May 2001; accepted 7 May 2001

Abstract

This study uses compositional analyses of garnet porphyroblasts to test a previously published microstructure-based model of garnet growth in the Fleur de Lys Supergroup. X-ray maps reveal significant compositional anomalies within garnet, including zoning reversals and steepened compositional gradients. These anomalies occur at the margin of the proposed first stage of garnet growth (G_1), and coincide with truncations of inclusion trails and changes in the inclusion assemblage. Intervals of reversed composition zoning and steepened compositional gradients across this boundary are interpreted to represent a hiatus in garnet growth, possibly accompanied by garnet consumption, during which changes in the garnet-forming reaction, *P–T* conditions and deformation kinematics occurred. The junction of the proposed second and third stages of garnet growth (G_2 and G_3) coincides with the transition between successive crenulation cleavages, without substantial microstructural truncations or changes in the inclusion assemblage. The G_2–G_3 boundary is generally marked by uninterrupted normal zoning, with subtle compositional anomalies in some samples. This boundary may in fact record continuous garnet growth, or alternatively mark a relatively short intra-orogenic pause in garnet growth with minimal affect on zoning patterns. Individual porphyroblasts with contrasting inclusion trail microstructures also have different zoning patterns, and this supports the previous recognition of contrasting growth histories between individual porphyroblasts. A combined structural–metamorphic model is presented that integrates the timing of garnet growth and foliation development, reaction history and the *P–T–t* path in the Fleur de Lys Supergroup.

Keywords: Chemical zoning; Fleur de Lys Supergroup; Garnet; Inclusion assemblage; Microstructure

1. Introduction

Microstructures preserved within porphyroblasts can be used to complement and commonly extend the structural history recorded in the rock matrix (e.g. Johnson, 1992; Aerden, 1995; Davis, 1995). Several recent studies have used microstructural timing criteria to distinguish multiple stages of porphyroblast growth (e.g. Jones, 1994; Spiess and Bell, 1996; Stallard, 1998). A useful test of the accuracy of these models is to generate compositional maps of the porphyroblasts and examine zoning trends across the proposed boundaries between successive growth stages. Previous studies have used compositional data to identify multiple growth stages in garnet porphyroblasts (e.g. Rumble and Finnerty, 1974; Karabinos, 1984; Grover et al., 1992), although in such studies compositional data have not been integrated with detailed microstructural analysis.

Garnet porphyroblasts in the Fleur de Lys Supergroup, Newfoundland, Canada, contain prominent, and commonly complex inclusion trails. Stallard (1998) used microstructural timing criteria to identify four stages of garnet growth (G_1–G_4) in the Fleur de Lys Supergroup, including up to three stages of growth recorded in a single porphyroblast. In this study, six garnet porphyroblasts, including five of the porphyroblasts presented by Stallard (1998), have been analysed to test for compositional anomalies across the margin of G_1 garnet growth, and across the G_2–G_3 growth-stage boundary. G_4 was identified not from microstructural discontinuities, but from timing relative to matrix foliations, and thus the G_3–G_4 boundary was not analysed.

The aim of this paper is to compare compositional and microstructural trends in garnet porphyroblasts from the Fleur de Lys Supergroup, and to test the conclusions of Stallard (1998), who proposed four stages of garnet growth

* Corresponding author. Current address: Institute of Geosciences, Shizuoka University, Shizuoka 422-8529, Japan. Tel.: +81-54-237-1111; fax: +81-54-238-0491.

E-mail address: aaron@se-geomail.sci.shizuoka.ac.jp (A. Stallard).

[1] Current address: Mineral Deposit Research Unit, Department of Earth and Ocean Sciences, University of British Columbia, Vancouver, BC, Canada.

0191-8141/02/$ - see front matter
PII: S0191-8141(01)00095-5

and contrasting growth histories in different garnet porphyroblasts based on a detailed microstructural study of these same samples.

2. Geological setting

The Fleur de Lys Supergroup consists dominantly of polydeformed upper greenschist to lower amphibolite facies schists with interlayered metabasalt and amphibolites (Fig. 1). Pre-porphyroblast assemblages were formed at an estimated 7.0–8.5 kbar and 450°C, and garnet porphyroblasts grew at an estimated 6.5 kbar and 550°C (Jamieson, 1990). The Supergroup is thought to represent a Late Proterozoic to Early Ordovician continental margin developed upon Grenvillian basement and buried by thrust sheets during the Ordovician Taconic Orogeny (Hibbard, 1983).

Cawood et al. (1994, 1995) distinguished two phases of deformation during the Taconic Orogeny related to accretion of the Dunnage Zone to the Laurentian margin (Taconian I) and final closure of the Iapetus Ocean (Taconian II). Full-scale collision between the Laurentian and Gondwana plates probably occurred during the Early Silurian Salinic Orogeny (Cawood et al., 1994).

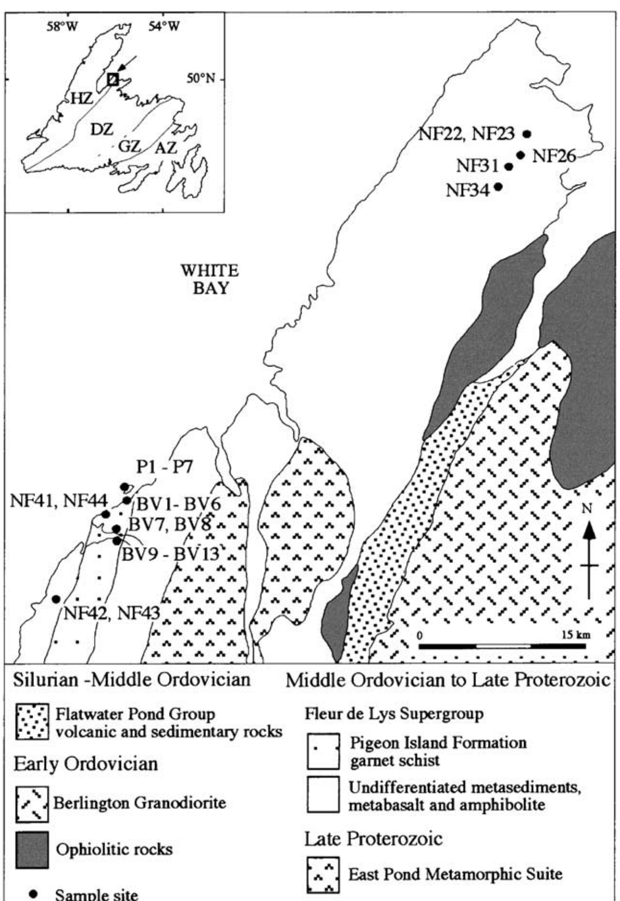

Fig. 1. Location map of the study area within Newfoundland, including sample localities and generalised geology (modified from Stallard, 1998; geology after Hibbard, 1983). HZ = Humber zone, DZ = Dunnage zone, GZ = Gander zone, AZ = Avalon zone.

3. Garnet porphyroblasts

3.1. Garnet growth history

Microstructure–porphyroblast relationships have been used to provide timing constraints on a succession of seven crenulation cleavages (S_1–S_7) and four stages of garnet growth (G_1–G_4) in the Fleur de Lys Supergroup (Stallard, 1998; Table 1; Fig. 2). The seven foliations were identified by overprinting relationships. S_1–S_5 were recognised within garnet porphyroblasts, S_5–S_6 within albite porphyroblasts, and S_4–S_7 within the matrix. Garnet porphyroblasts grew episodically through four growth stages, and growth during successive stages did not occur on all pre-existing porphyroblasts (Table 1). This resulted in contrasting growth histories amoung individual garnet porphyroblasts from the same outcrop. A summary sketch illustrating the relationships between the different foliations and garnet growth stages is shown in Fig. 2.

3.1.1. G_1 garnet growth

Garnet porphyroblasts commonly preserve the idioblastic outline of an early stage of garnet growth (G_1; e.g. Fig. 3). G_1 growth contains a distinctive inclusion assemblage dominated by rutile needles with additional quartz, chloritoid, chlorite, allanite, apatite, and white mica. At least two foliations (S_1 and S_2) are outlined by inclusion trails within the G_1 portion of garnet porphyroblasts and these represent the earliest deformation microstructures preserved within the Fleur de Lys Supergroup (Figs. 2d and 3f). The boundary between G_1 and subsequent growth stages is marked by microstructural truncations, changes in inclusion mineralogy, and adjacent quartzose strain shadows that are entrapped by subsequent garnet growth (Figs. 2c and d and 3).

3.1.2. Garnet growth subsequent to G_1

Garnet porphyroblasts contain two inclusion trail foliations (S_3 and S_4) intermediate in age between the G_1 growth stage and the matrix foliations S_5 and S_6 (Figs. 2 and 3). S_3 and S_4 are mainly outlined by quartz inclusions, with minor epidote, apatite, white mica and ilmenite. S_3 is preserved only in porphyroblasts, whereas S_4 is also preserved in the adjacent matrix (Fig. 2). Two discrete stages of garnet growth (G_2 and G_3) are approximately synchronous with the formation of S_3 and S_4 (Table 1). A number of garnet porphyroblasts contain straight inclusion trails continuous with, and of the same orientation as, the dominant matrix S_5 schistosity (e.g. Fig. 3e). This indicates garnet growth subsequent to S_5, and this late stage of growth is termed G_4 (Table 1; Fig. 2). The matrix mineral assemblage

Table 1
Summary microstructural history of the Fleur de Lys Supergroup. (a) History of foliations and timing of garnet growth. (b) Contrasting growth histories recorded by four garnet porphyroblasts from the Fleur de Lys Supergroup, as proposed by Stallard (1998). Photomicrographs and accompanying line diagrams of the four porphyroblasts are provided in Fig. 3, and the zoning patterns of each porphyroblast are presented in Figs. 4–6. Modified from Stallard (1998)

(a)	Foliation	Foliation description	Timing of garnet growth
	S_7	Late incipient crenulation cleavage. Matrix only	
	S_6	Crenulation cleavage developed in matrix to varying intensities	
			| G_4
	S_5	Layer parallel, dominant matrix foliation. Preserved also inside garnet porphyroblasts (linear trails)	
			| G_3
	S_4	Inside garnet, also rarely preserved in matrix adjacent to garnet porphyroblasts and in microlithons between S_5 foliation seams	
			| G_2
	S_3	Preserved only inside garnet porphyroblasts	
			| G_1
	S_1, S_2	At least two foliations inside early garnet core. Preserved only inside garnet porphyroblasts	

(b)	Garnet growth stage	Foliation overgrown by garnet	BV6 030 (Fig. 3b)	BV9 030L (Fig. 3a)	BV9 030S (Fig. 3c)	BV5 120 (Fig. 3e)
	G_1	S_1, S_2	●	●		●
	G_2	S_3		●	●	
	G_3	S_4	●	●	●	
	G_4	S_5				●

includes quartz, albite, staurolite, three textural generations of white mica (Jamieson and Vernon, 1987), ilmenite, epidote, biotite, chlorite, carbonate, graphite and garnet.

4. Compositional data

Six garnet porphyroblasts (see Fig. 3) have been analysed to test for compositional anomalies across the proposed G_1 boundary and G_2–G_3 growth-stage boundaries. Analysis is based on X-ray maps of three of the porphyroblasts and line transects across all six garnet (Figs. 4–6).

X-ray maps were produced on a Cameca SX50 electron microprobe housed at the Department of Geosciences, University of Massachusetts. The maps involve 512 × 512 stage scan analyses made with WDS spectrometers, taken at 125 nA beam current, 15 kV and 80 ms count time. Line transects consist of 64 or 128 analysis points typically at 20–30 μm spacing, which were acquired using EDS techniques using a JOEL JXA-840A microprobe housed at the Advanced Analytical Centre, James Cook University, operating at 15 kV and 10 nA, with 20 s count times. Analyses of inclusions and adjacent matrix minerals encountered during each line traverse have been removed from the data. Transects are three-point moving averages of X_{grs}, X_{alm} and X_{sps}. Concentrations of wt% MgO are shown on the colour maps derived from WDS analysis, but these values are below the level of precision of the EDS analysis, resulting in a large scatter of values, and hence X_{pyr} is not plotted on the EDS traverses. Representative analyses of the cores and rims of analysed porphyroblasts are shown in Table 2.

4.1. Description of compositional data

4.1.1. Boundary between G_1 and subsequent growth stages

4.1.1.1. Garnet BV6 030 and BV6 170 (Fig. 4) The G_1 portion of each porphyroblast contains a positive X_{grs} spike, and negative X_{alm} and X_{sps} spikes (Fig. 4e and f, interval *a*; in this section, interval a, b, etc. refer to indicated sections of line transects). The proposed boundary between successive growth stages is marked by a sharp decrease in X_{grs} and increase in X_{alm} and X_{pyr} (Fig. 4), and is generally preceded by an interval of reversed compositional zoning (e.g. shaded grey area in Fig. 4f). The G_3 growth in both

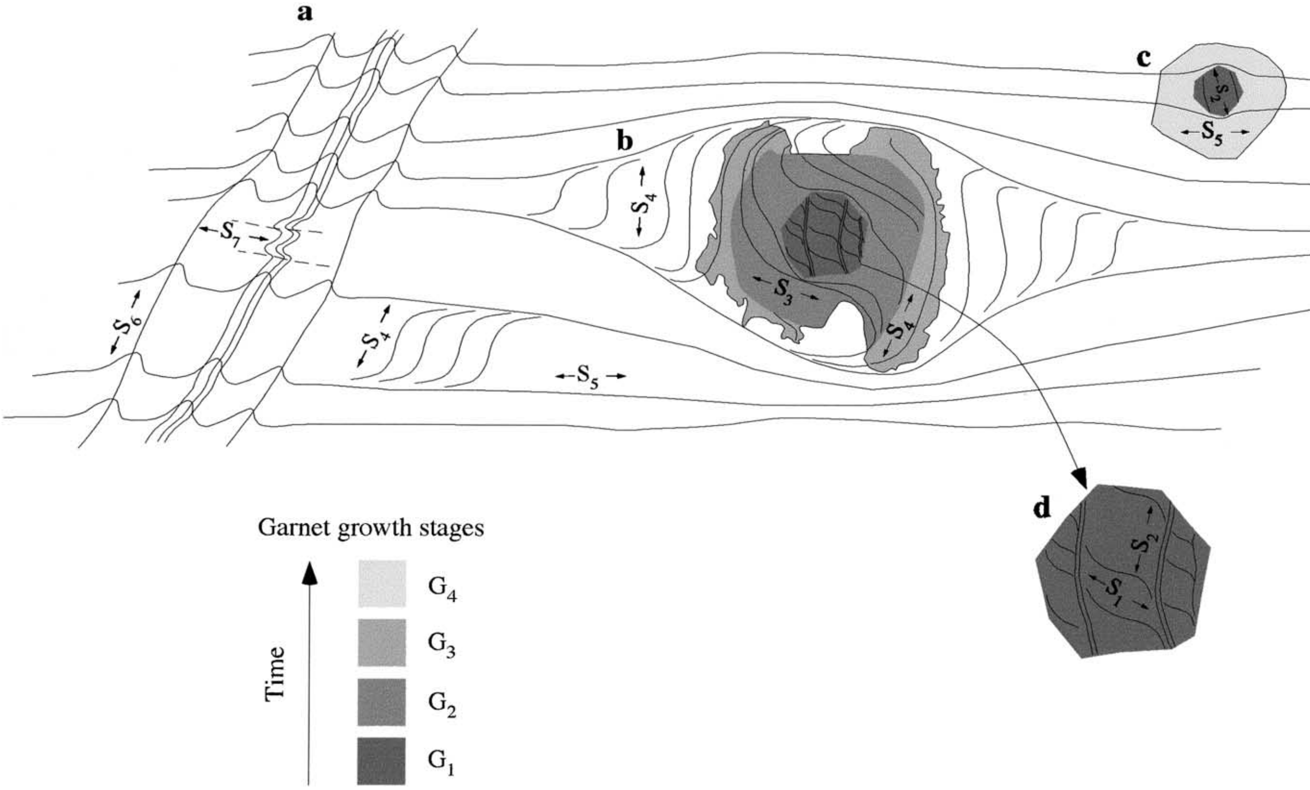

Fig. 2. Summary sketch illustrating the spatial and temporal relationships between the seven crenulation cleavages and four stages of garnet growth identified in the Fleur de Lys Supergroup, as proposed by Stallard (1998). (a) Overprinting matrix foliations. (b) S_4 preserved both in the matrix adjacent to garnet porphyroblasts, and in porphyroblast rims. Also S_3 preserved inside garnet porphyroblasts (e.g. Fig. 3a). (c) Garnet porphyroblast consisting of G_1 and G_4 growth stages, without intervening G_2 and G_3 stages (e.g. Fig. 3e). (d) G_1 growth over S_1 and S_2 crenulation cleavages outlined by rutile needles (e.g. Fig. 3f).

porphyroblasts (interval *b*) contains a narrow interval of reversed compositional zoning in the outer rim.

4.1.1.2. Garnet BV1 030 and BV5 120 (Fig. 5) Within the proposed first stage of garnet growth (see Fig. 5a and interval *a* on line traverses), the X_{sps} profile is dominated by a series of peaks and troughs defining oscillations within an approximately subhorizontal overall trend. The X_{sps} profile is complex, and resembles the anomalous X_{grs} profiles described by Chernoff and Carlson (1997). At the proposed boundary between the two growth stages (dashed vertical lines), there occurs a large positive spike in X_{sps} and a narrow interval of reversed X_{grs} and X_{alm} zoning. An interval of normal growth zoning succeeds the proposed growth stage boundary (interval *b*). The porphyroblast margin (BV1 030 interval *c*) is marked by zoning reversals in X_{sps} and X_{alm}.

4.1.2. Boundary between G_2 and G_3 growth stages

4.1.2.1. Garnet BV9 030L (Fig. 6) The compositional maps and line transects across BV9 030L reveal typical X_{alm}, X_{grs} and X_{sps} zoning profiles, with suggestions of X_{alm} and X_{grs} anomalies at the G_1–G_2 boundary (Fig. 6e), although these zoning anomalies are not apparent on the detailed transect (Fig. 6f). The transect across the proposed G_1–G_2 boundary (Fig. 6f) reveals asymmetric profiles with respect to the positioning of the G_1–G_2 boundary. Subtle peaks in X_{alm}, and a negative spike in X_{grs} composition coincide with the G_1–G_2 boundary (dashed vertical lines), although these features are largely indistinguishable in magnitude and geometry from similar peaks and spikes in other parts of the profile. A second detailed transect was positioned to intersect the proposed boundary between the G_2 and G_3 growth stages (Fig. 6g), but does not reveal any zoning anomalies. A spike in X_{grs} occurs at the very margin of the porphyroblast.

4.1.2.2. Garnet BV9 030S (Fig. 6h and i) The full transect (Fig. 6h) displays a gradual depletion in X_{grs}, enrichment in X_{alm}, and typical steep depletion of X_{sps} from core to rim. The right side edge of the profile displays an anomalous horizontal trend distinct from the rest of the profile. A detailed transect across the proposed G_2–G_3 boundary revealed no detectable compositional anomalies (Fig. 6i).

5. Interpretation of compositional data

Growth zoning profiles within garnet porphyroblasts typically involve X_{alm} and X_{pyr} enrichment from core to rim, and a corresponding depletion in X_{sps} and X_{grs} (e.g. Spear, 1993).

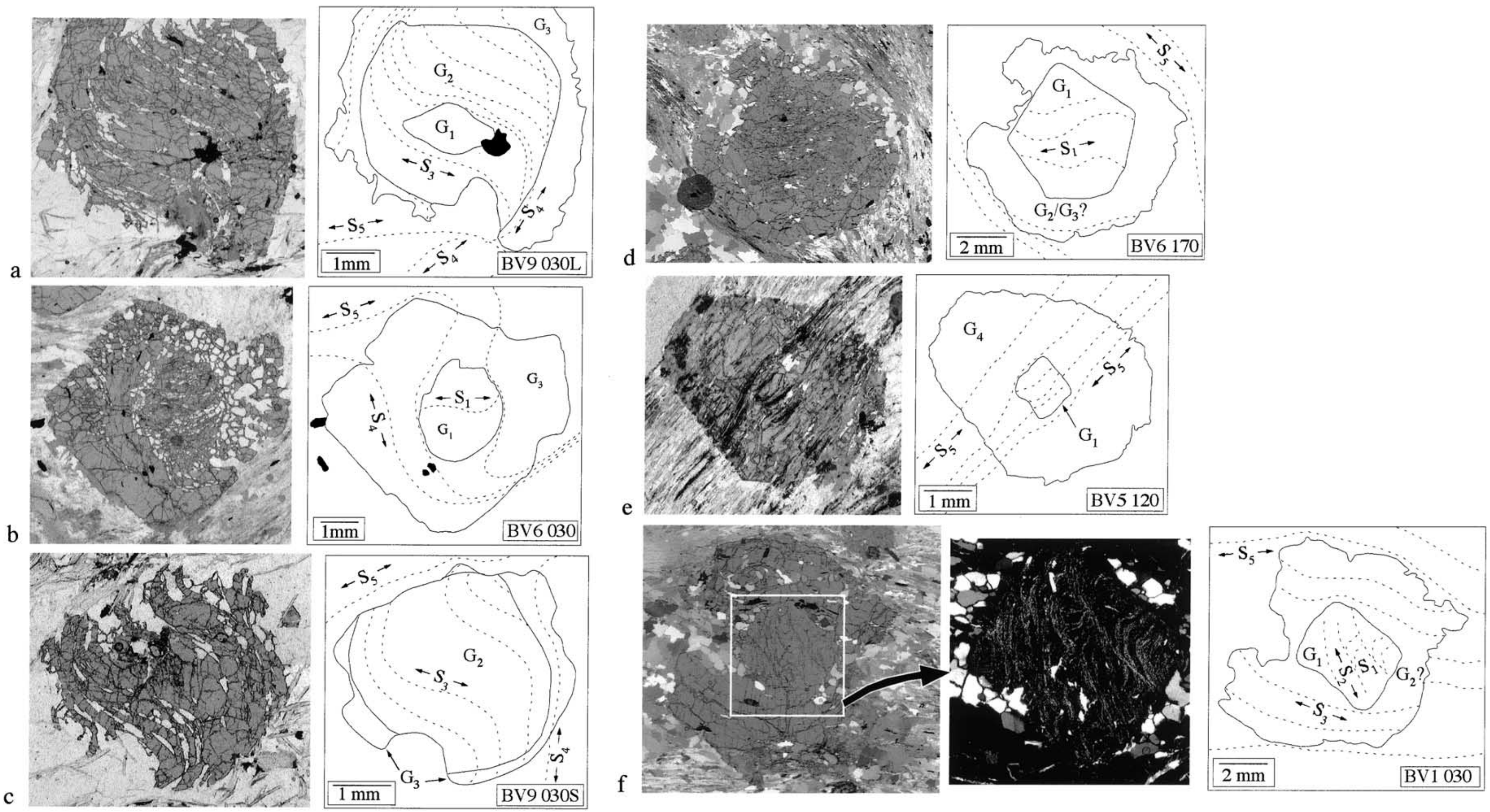

Fig. 3. Photomicrographs and accompanying line diagrams of garnet porphyroblasts analysed in this study. Dashed lines indicate the trace of inclusion trails and matrix foliations. Solid lines within the porphyroblasts indicate boundaries between growth stages (e.g. G_1, G_2), as proposed by Stallard (1998). Sample numbers correspond to those shown in Fig. 1. Porphyroblasts shown in Fig. 3a and c are from the same sample. Photomicrograph of central portion of garnet in Fig. 3f is crossed polarised light.

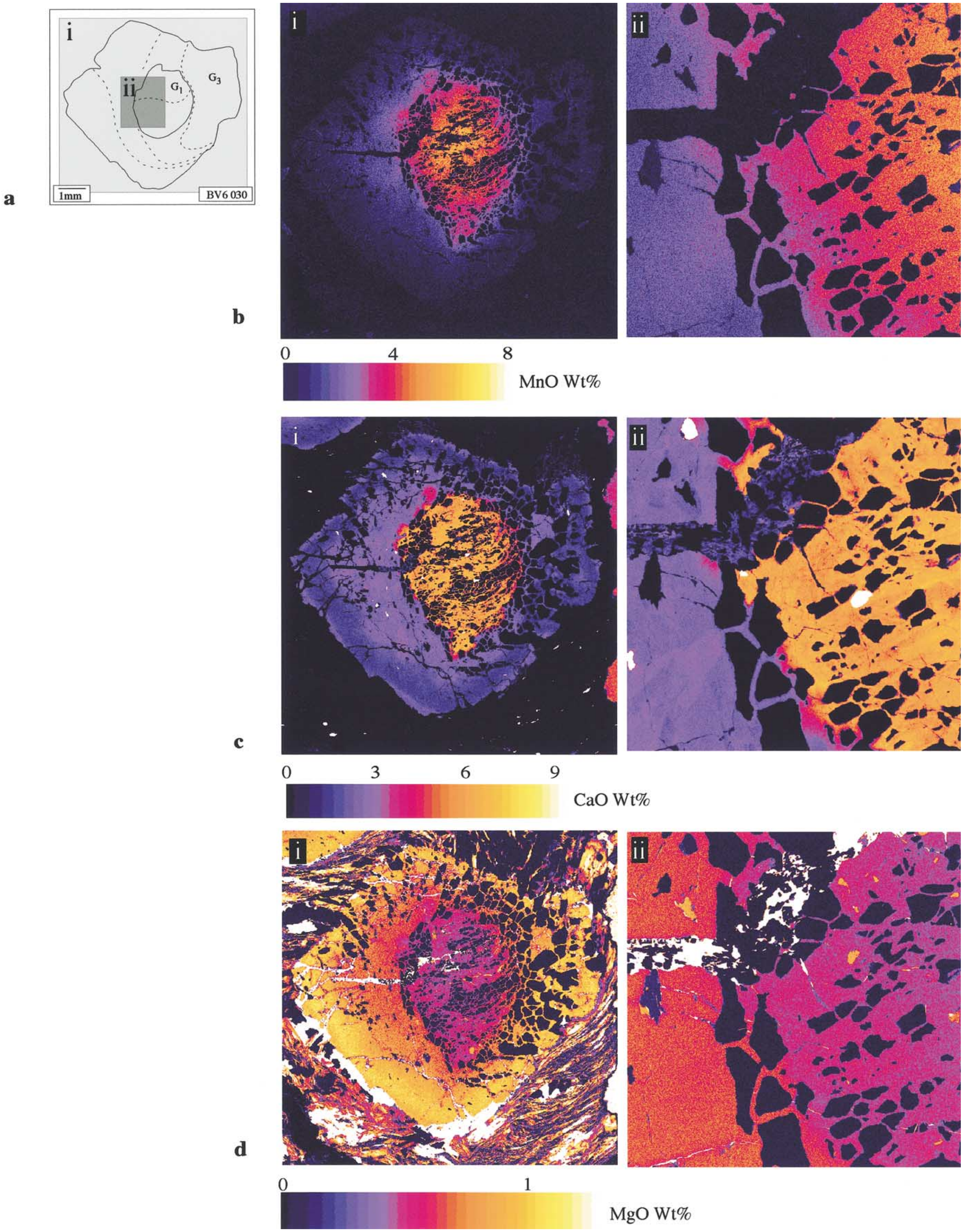
a
i
ii
G1
G3
1mm
BV6 030
b
i
ii
0
4
8
MnO Wt%
c
i
ii
0
3
6
9
CaO Wt%
d
i
ii
0
1
MgO Wt%

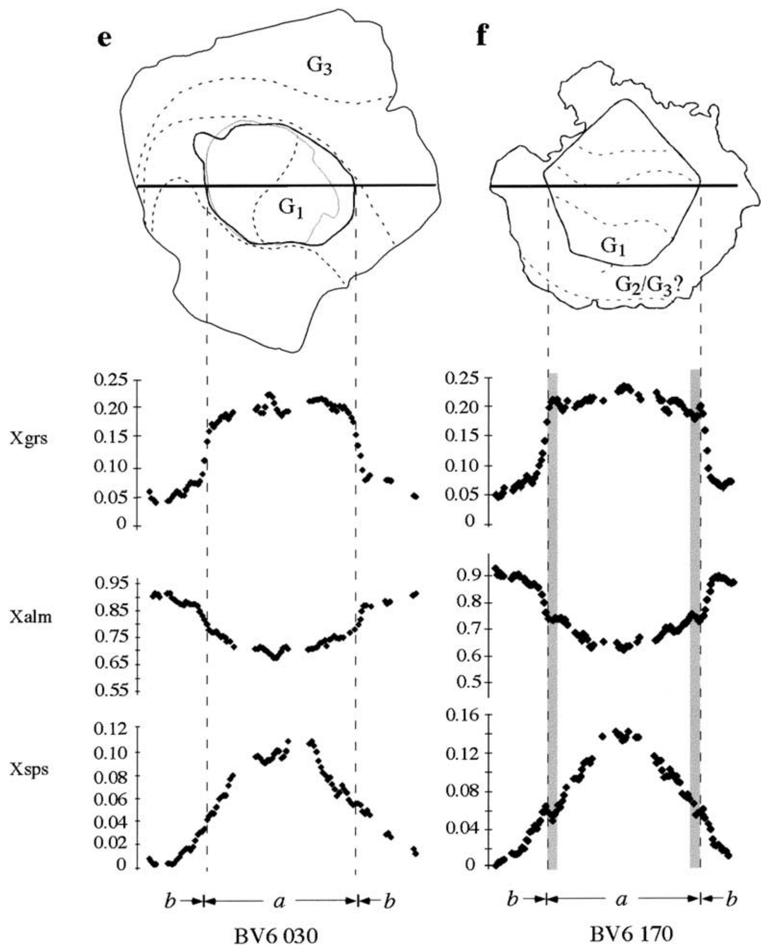

Fig. 4. (*continued*)

Variations from this typical profile have been observed in this and previous studies (e.g. Hames and Menard, 1993; Chernoff and Carlson, 1997), and include zoning reversals (e.g. X_{sps} profile in Fig. 4f), steepened compositional gradients (e.g. X_{grs} profile in Fig. 4e), and compositional discontinuities. The origin of typical and atypical composition zonation is generally attributed to one or more of the following processes: (a) preferential fractionation of certain elements into early garnet resulting in depletion of those elements in the matrix (e.g. Cygan and Lasaga, 1982); (b) changes in the garnet–matrix mineral partition coefficients due to changes in *P–T* conditions (e.g. Spear, 1993); (c) syn-growth reaction changes (e.g. Chernoff and Carlson, 1997); (d) re-equilibration of cations by intracrystalline diffusion (e.g. Ikeda, 1993); (e) interaction with a metasomatic fluid (e.g. Young and Rumble, 1993); and (f) limitations of reaction rates at the mineral–matrix interface (e.g. Carlson, 1989).

5.1. G_1 growth and the boundary between G_1 and subsequent growth stages (Figs. 4 and 5)

The first growth stage (G_1; interval *a* on transects) in garnet BV6 030 and BV6 170 (Fig. 4e and f) involved largely typical growth zoning, but samples BV1 030 and BV5 120 (Fig. 5e and f) contain anomalously sub-horizontal profiles dominated by oscillations in the garnet zoning. Despite the evidence of oscillatory zoning evident in

Fig. 4. Compositional analyses of garnet porphyroblasts BV6 030 and BV6 170. (a) Line drawing of garnet BV6 030. Grey boxes and Roman numerals indicate area of analysis of corresponding colour maps (b–d). (e and f) Line transects across porphyroblasts BV6 030 and BV6 170. Horizontal lines across porphyroblast outlines indicate the position of each transect. Dashed vertical lines indicate the position on the transect of the proposed boundary between the first stage of garnet growth (G_1) and subsequent growth stages. Shaded area highlights interval of reversed compositional zoning. Porphyroblast outlines have been rotated (from orientation in Fig. 3) in order to position profiles horizontal upon the page. Note that the compositionl G_1 boundary in BV6 030 (black line) differs slightly from the microstructural boundary (grey line). This is due to uncertainties in the position of the microstructural boundary in those parts of the garnet where inclusions are less concentrated. The X-ray map clearly reveals the location of the boundary in those parts of the garnet with fewer inclusions.

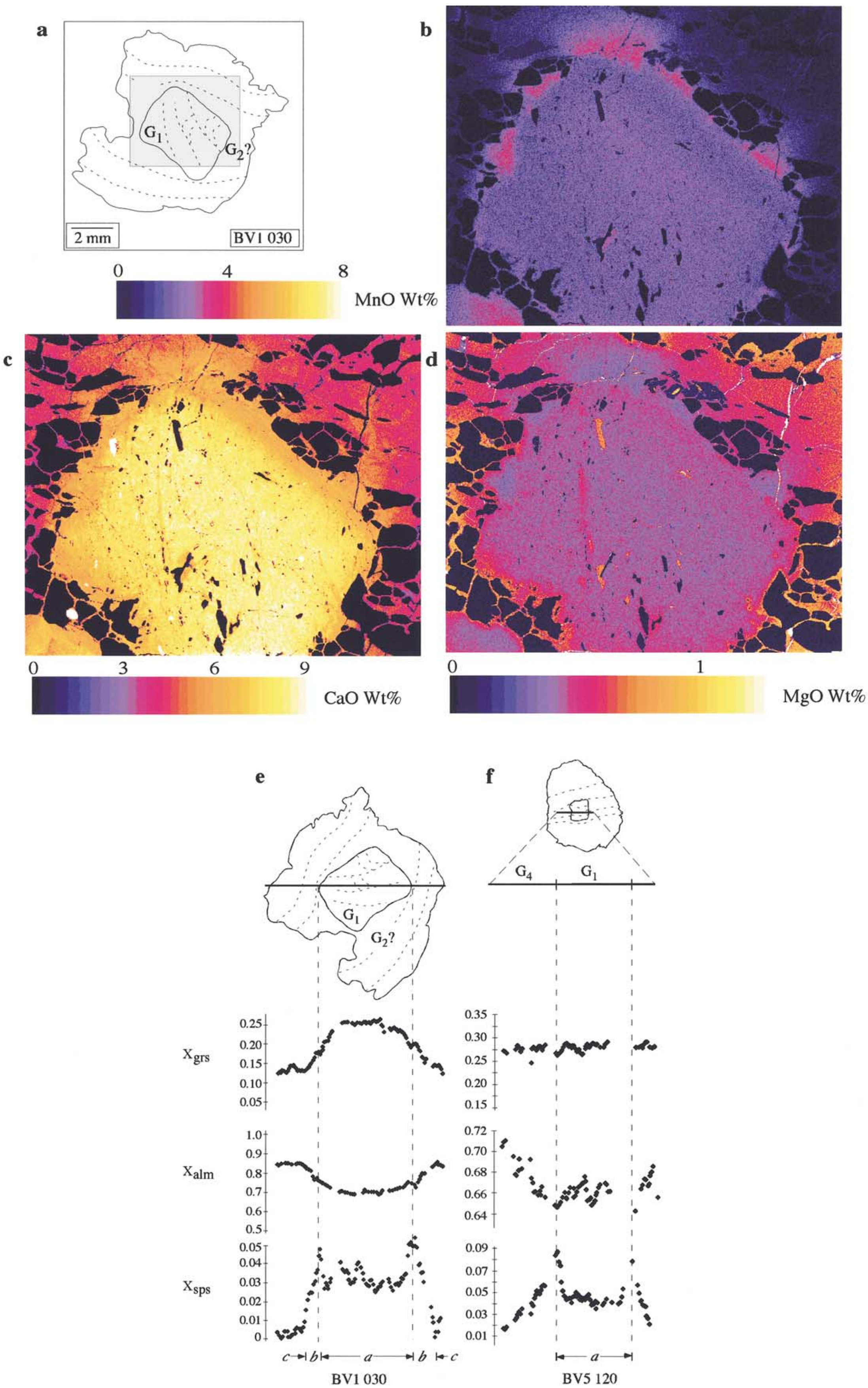
a
G1
G2?
2 mm
BV1 030
b
0
4
8
MnO Wt%
c
d
0
3
6
9
CaO Wt%
0
1
MgO Wt%
e
G1
G2?
f
G4
G1
Xgrs
0.25
0.20
0.15
0.10
0.05
Xalm
1.0
0.9
0.8
0.7
0.6
0.5
Xsps
0.05
0.04
0.03
0.02
0.01
0
0.35
0.30
0.25
0.20
0.15
0.72
0.70
0.68
0.66
0.64
0.09
0.07
0.05
0.03
0.01
c b a b c
a
BV1 030
BV5 120

published composition profiles of garnet porphyroblasts (e.g. Blackburn and Navarro, 1977; fig. 2 of Irwin, 1994; fig. 1 of Chernoff and Carlson, 1997) the phenomenon has not received significant attention as a growth process in garnet porphyroblasts produced during regional metamorphism. The oscillations may have resulted from a degree of self-organisation in the growing porphyroblasts (e.g. Reeder et al., 1990), or the coalescence of multiple nuclei (Daniel and Spear, 1998). The consistent association between oscillatory zoning and subhorizontal zoning patterns may be significant, as the processes that produce the oscillatory zoning may also act to negate the development of normal depletion or enrichment zoning. The position of the change from oscillatory to normal X_{sps} zoning coincident with the G_1 margin suggests the X_{sps} profiles are not simply the result of a section cut at a distance from the porphyroblast core.

Zoning reversals at the G_1 margin are interpreted to represent compositional modification of the garnet edge during a hiatus in garnet growth, or a period of garnet consumption (e.g. Florence and Spear, 1993; Lang, 1996). This interpretation is supported by the occurrence of microstructural truncations and changes in inclusion mineralogy coincident with the position of the proposed hiatus in growth (see Fig. 3; Stallard, 1998). Reversals in the typical zoning trends of the major cations are commonly observed in the outer rim of garnet porphyroblasts, and this is usually attributed to retrograde resorption of garnet to produce biotite or chlorite (Karabinos, 1984; Ikeda, 1993). Zoning reversals within the interior of a porphyroblast, such as that recorded at the G_1–G_2 boundary (e.g. Fig. 4f), may represent compositional modification of the garnet rim, as described above, during a hiatus in garnet growth, possibly accompanied by garnet consumption, and followed by a second stage of garnet growth and resumption of normal zoning (e.g. Karabinos, 1984; Irwin, 1994).

The steepened gradients in X_{alm} and X_{grs} concentrations (BV6 030 and BV6 170) and spikes in X_{sps} (BV1 030 and BV5 120) at the G_1 margin are interpreted to represent a hiatus in garnet growth, a change in the garnet-forming reaction, and/or a change in P–T conditions (see Section 6 for metamorphic model; Rumble and Finnerty, 1974; Karabinos, 1984; Grover et al., 1992; Hickmott and Spear, 1992; Erambert and Austrheim, 1993; Irwin 1994; Spiess and Bell, 1996). This may signify multiple garnet-growth episodes within a continuous metamorphic event, or growth during successive distinct metamorphic cycles.

The zoning reversals in the outer rims of the analysed porphyroblasts (e.g. Fig. 4e) are interpreted to represent post-growth intracrystalline diffusion and re-equilibration of the garnet edge with matrix cation concentrations.

The lack of compositional variation across the proposed G_1–G_2 boundary in garnet BV9 030L (Fig. 6) suggests this may not be a comparable feature to those boundaries shown in Figs. 4 and 5. The proposed G_1 growth in this sample may therefore be a previously unrecognised growth stage, or alternatively represent continuous garnet growth.

5.2. Boundary between G_2 and G_3 (Fig. 6)

The boundary between the proposed G_2 and G_3 growth stages is marked by subtle compositional anomalies in garnet BV9 030L (Fig. 6g), but records no anomalies in garnet BV9 030S (Fig. 6i). The general absence of zoning anomalies in Fig. 6 suggests that either garnet growth was continuous across the proposed G_2–G_3 boundary, or that a relatively minor hiatus in garnet growth occurred without disruption to the zoning pattern.

6. Discussion

6.1. Implications of compositional data for previous microstructure-based model of garnet growth in the Fleur de Lys Supergroup

Five of the six garnet porphyroblasts analysed in this study contain proposed G_1 growth stages, and with the exception of BV9 030L (Fig. 6), the porphyroblasts contain compositional anomalies at the G_1 margin. These anomalies are coincident with microstructural truncations and changes in the inclusion assemblage, and are consistent with the previously published interpretation of the G_1 margin as a hiatus in garnet growth, possibly accompanied by garnet consumption (Table 1; Stallard, 1998). The proposed G_2–G_3 boundary however, is marked by minor anomalies and even uninterrupted normal zoning, and thus it is uncertain as to whether this boundary represents a pause in garnet growth or continuous growth across the boundary. Spiess and Bell (1996) also analysed zoning patterns across growth boundaries in garnet porphyroblasts, and found that zoning truncations are only recorded at growth-stage boundaries that are accompanied by garnet consumption. Within the Fleur de Lys Supergroup, the compositional data is inconclusive as to whether the G_2–G_3 boundary records a hiatus in garnet growth.

The compositional data also provides insight into the proposed contrasting growth histories of individual garnet porphyroblasts listed in Table 1. Garnet BV9 030L and BV9

Fig. 5. Compositional analyses of garnet porphyroblasts BV1 030 and BV5 120. (a) Line drawing of garnet BV1 030. Grey box indicates area of analysis of corresponding colour maps (b–d). (e and f) Line transects across porphyroblasts BV1 030 and BV5 120. Horizontal lines across porphyroblast outlines indicate the position of each transect. Dashed vertical lines indicate the position on the transect of the proposed boundary between the first stage of garnet growth (G_1) and subsequent growth stages. Porphyroblast outlines have been rotated (from orientation in Fig. 3) in order to position profiles horizontal upon the page.

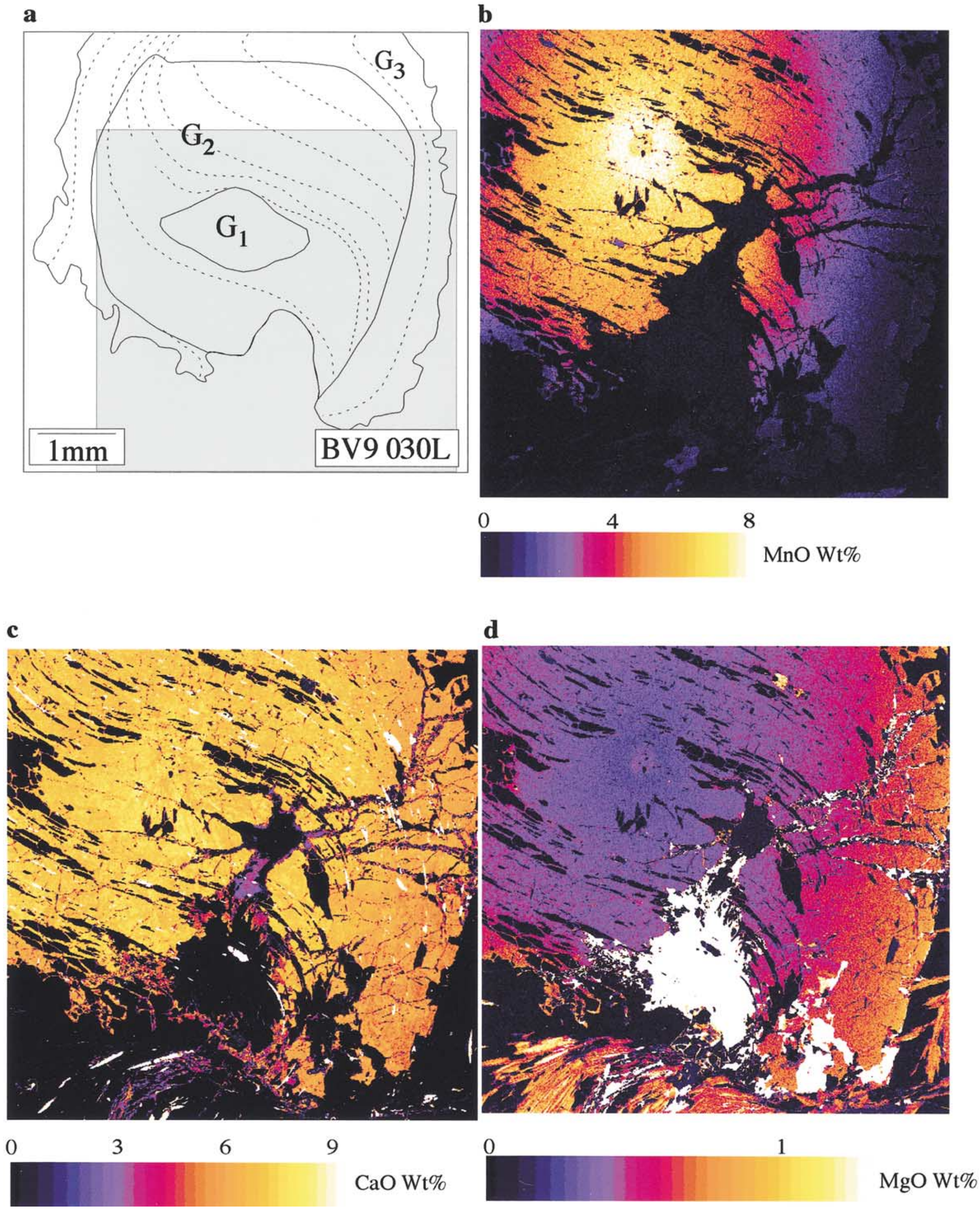

Fig. 6. Compositional analyses of garnet porphyroblasts BV9 030L and BV9 030S. (a) Line drawing of garnet BV9 030L. Grey box indicates area of analysis of corresponding colour maps (b–d). (e–g) Line transects across garnet BV9 030L, including full transect (e), and detailed transects across the proposed G_1–G_2 boundary (f) and G_2–G_3 boundary (g). The transect in (e) consists of two slightly unparallel half transects in order to avoid intersecting areas of concentrated quartz inclusions. (h and i) Line transects across garnet BV9 030S, including full transect (h), and detailed transect across proposed G_2–G_3 boundary (i). Horizontal lines across porphyroblast outlines indicate the position of each transect. Dashed vertical lines indicate the position on the transect of the proposed boundary between growth stages. Porphyroblast outlines have been rotated (from orientation in Fig. 3) in order to position profiles horizontal upon the page.

030S grew during the G_1 (BV9 030L only), G_2 and G_3 growth stages, and show similar zoning profiles (Fig. 6e and h). These profiles contrast with the zoning patterns in garnet BV6 030 (Fig. 4), which grew during G_1 and G_3, and BV5 120 (Fig. 5f), which grew during G_1 and G_4. The varied growth zoning profiles in Figs. 4–6 are consistent with the interpretations of Stallard (1998) that different porphyroblasts in the Fleur de Lys Supergroup grew at different

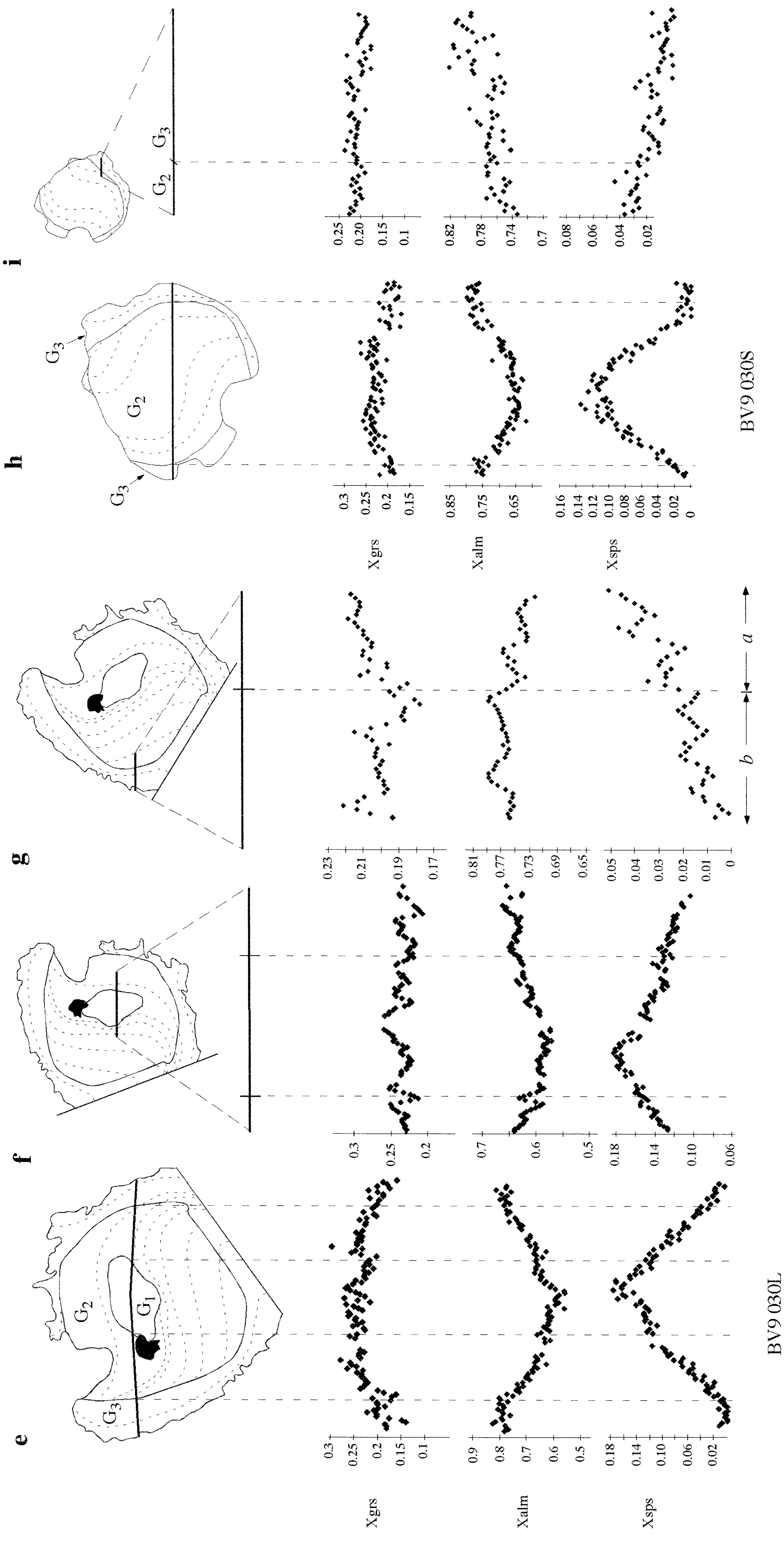

Fig. 6. (*continued*)

Table 2
Representative compositional analyses of the cores and rims of the six garnet porphyroblasts shown in Fig. 3

	BV1 030		BV5 120		BV6 030		BV6 170		BV9 030L			BV9 030S	
	Core	Rim	Core	Rim	Core	Rim	Core	Rim	Core	Med	Rim	Core	Rim
SiO_2	38.10	37.80	37.50	37.30	37.00	36.60	38.00	37.60	37.10	37.40	37.00	36.70	36.70
TiO_2	0.00	0.10	0.21	0.24	0.00	0.15	0.05	0.35	0.07	0.24	0.32	0.18	0.00
Al_2O_3	20.10	20.20	20.60	20.70	20.90	20.80	20.90	20.40	20.70	20.10	20.10	20.30	20.30
FeO	31.00	35.90	29.20	31.30	30.20	39.40	31.00	35.90	27.00	31.00	34.20	30.20	34.40
CaO	9.03	4.06	9.56	8.94	6.98	0.88	6.21	2.01	8.18	7.76	6.41	7.95	6.21
MgO	0.41	1.45	1.22	1.03	0.82	2.07	1.13	1.25	0.51	1.00	0.48	0.53	1.32
MnO	1.26	0.17	1.30	0.53	3.56	0.13	2.46	0.82	6.05	2.64	0.21	3.42	0.08
Cr_2O_3	0.00	0.00	0.00	0.00	0.00	0.00	0.00	0.00	0.00	0.07	0.07	0.04	0.10
Total	99.90	99.68	99.59	100.04	99.46	100.03	99.75	98.33	99.61	100.21	98.79	99.32	99.11
Si	6.14	6.12	6.01	5.98	6.00	5.97	6.11	6.16	6.00	6.03	6.07	5.99	5.99
Ti	0.00	0.01	0.02	0.03	0.00	0.02	0.01	0.04	0.01	0.03	0.04	0.02	0.00
Al	3.82	3.86	3.90	3.91	4.00	3.99	3.96	3.94	3.94	3.82	3.88	3.90	3.91
FeO	4.17	4.85	3.91	4.20	4.09	5.37	4.17	4.91	3.65	4.18	4.68	4.12	4.69
Ca	1.55	0.70	1.64	1.53	1.21	0.15	1.07	0.35	1.41	1.34	1.12	1.39	1.08
Mg	0.10	0.35	0.29	0.25	0.20	0.50	0.27	0.30	0.12	0.24	0.11	0.13	0.32
Mn	0.17	0.02	0.18	0.07	0.49	0.02	0.33	0.11	0.83	0.36	0.03	0.47	0.01
Cr	0.00	0.00	0.00	0.00	0.00	0.00	0.00	0.00	0.00	0.01	0.01	0.00	0.01
Total	15.95	15.91	15.95	15.98	15.99	16.02	15.91	15.82	15.96	16.01	15.94	16.02	16.02
Pyrope	1.64	5.89	4.84	4.07	3.31	8.32	4.64	5.37	2.04	3.93	1.97	2.11	5.25
Almandine	69.54	81.85	64.98	69.36	68.31	88.84	71.33	86.43	60.65	68.28	78.66	67.42	76.80
Spessartine	2.86	0.39	2.93	1.19	8.16	0.30	5.73	2.00	13.76	5.89	0.49	7.73	0.18
Grossular	25.95	11.86	27.25	25.38	20.23	2.54	18.31	6.20	23.54	21.90	18.89	22.74	17.76

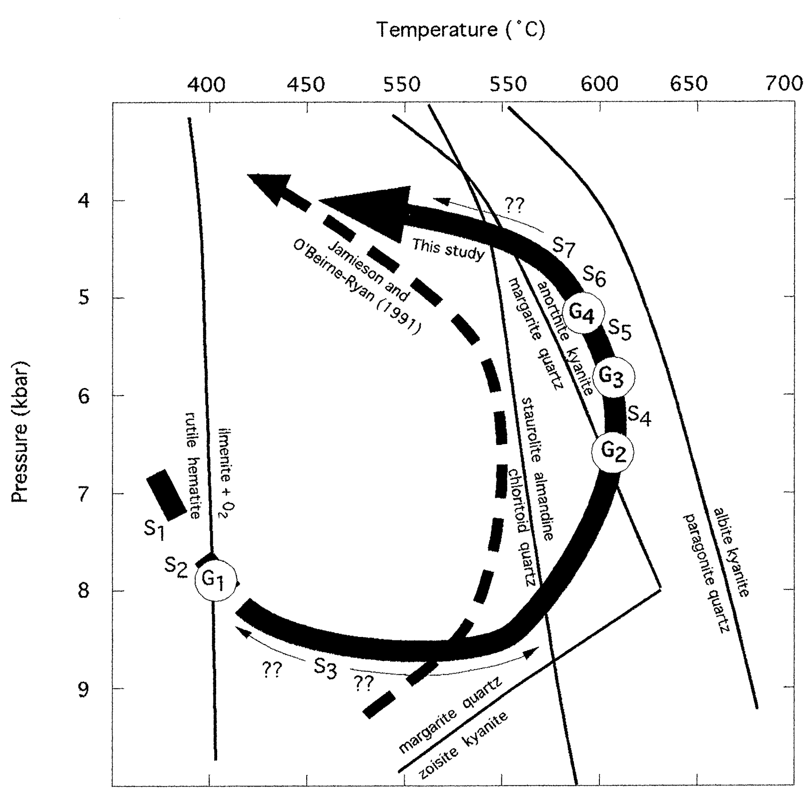

Fig. 7. P–T diagram, Fleur de Lys Supergroup, illustrating reactions, P–T–t path, timing of garnet growth, and foliation development. Reaction boundaries are from Jamieson (1990), and were calculated using Ge0-CALC (Brown et al., 1988), assuming $a_{H20} = 1$. P–T–t path modified from that of Jamieson (1990); Jamieson and O'Beirne-Ryan (1991).

stages in the metamorphic history, and therefore contain contrasting growth histories (Table 1).

6.2. An integrated model of structure and metamorphism in the Fleur de Lys Supergroup

The garnet zoning profiles and inclusion trail microstructures described in this study can be better understood in the context of the reaction history and P–T path recorded by the samples. Fig. 7 shows an intergrated metamorphic–structural model for the Fleur de Lys supergroup, including an interpreted P–T–t path, and timing of garnet growth and foliation development. The P–T–t path is based on that of Jamieson (1990) and Jamieson and O'Beirne-Ryan (1991), although it is modified to be consistent with the data presented in this study. Changes in the mineral assemblage preserved as inclusions in growth stages G_1 to G_4, and recorded by matrix minerals, provide constraints on the P–T–t path and timing of garnet growth. The key changes in the mineral assemblage are the loss of chloritoid, rutile and margarite at the G_1–G_2 boundary. None of these minerals occur in the matrix. These trends can be explained by the following reactions, which are largely derived from Jamieson (1990). Chloritoid was consumed during G_1 garnet growth by the garnet-forming reaction:

$$\text{chloritoid} + \text{biotite} + H_2O = \text{garnet} + \text{chlorite} \quad (1)$$

or

$$\text{chloritoid} + \text{biotite} + \text{quartz} = \text{garnet} + \text{muscovite} + H_2O \quad (2)$$

Following consumption of chloritoid at the G_1–G_2 boundary, post-G_1 garnet growth was by the following reaction

$$\text{chlorite} + \text{muscovite} + \text{quartz} = \text{garnet} + \text{biotite} + H_2O \quad (3)$$

The conversion of rutile to ilmenite across the G_1–G_2 boundary is explained by the reaction

$$\text{rutile} + \text{hematite} = \text{ilmenite} + O_2 \quad (4)$$

And likewise consumption of margarite is by

$$\text{margarite} + \text{quartz} = \text{anorthite} + \text{kyanite} + H_2O \quad (5)$$

The presence of rutile inclusions within G_1 garnet constrains G_1 growth to near the rutile–ilmenite transition, prior to the loss of rutile. Garnet growth at such low temperatures is not typically predicted, and relies upon a strong partitioning of MnO and to a lesser degree CaO into garnet. The contrasting inclusion assemblages between G_1 and G_2 constrain each stage of garnet growth to different points on the P–T path. Margarite, rutile and chloritoid inclusions have not been identified in post-G_1 garnet, and thus garnet growth subsequent to G_1 must post-date the relevant reactions that consume these minerals. In this way, the timing of each garnet growth stage is constrained relative to the reaction history and P–T–t path (Fig. 7). The foliations (S_1–S_7) are also plotted on the P–T–t path, as the timing of foliation development relative to garnet growth has already been proposed (Table 1a). As discussed earlier, it is uncertain as to whether the proposed G_2, G_3 and G_4 stages of garnet growth are separated by pauses in growth, or whether they represent continuous garnet growth that spans the development of multiple foliations. Despite this uncertainty, the relative timing of G_2, G_3 and G_4 is well constrained and thus they are plotted separately in Fig. 7 to illustrate timing relative to foliations.

The garnet zoning patterns presented in Figs. 4 and 5 can be further interpreted in terms of the reaction history and garnet growth patterns depicted in Fig. 7. The abrupt compositional changes across the G_1–G_2 boundary reflect multiple reactions and up to 200°C difference in temperature between the two growth stages (Fig. 7). For instance, during normal continuous garnet growth, the X_{grs} component in garnet is likely to steadily diminish towards the garnet rim as accessory epidote/clinozoizite and/or calcite is consumed during continuous prograde reactions in the KFMASH (+Ca) system. The effect of pausing garnet growth between G_1 and G_2 is that resumption of garnet growth during G_2 occurs at much lower X_{grs} than the final stages of G_1 growth (e.g. Fig. 4). The same process is able to explain the steep X_{alm} gradients shown in Fig. 4.

By contrast, the sharp spikes in X_{sps} at the margin of G_1 in Fig. 5 are not easily explained in terms of reaction changes or variable Mn partitioning between different phases, as none of the inclusions analysed within G_1 are suitable Mn sinks. Chloritoid inclusions within G_1 contain between only 0.04 and 0.68 wt% Mn, chlorite between 0.01 and 0.08 wt% Mn, and Mn-epidote has not been found. The steep positive X_{sps} gradient at the margin of interval *a* may represent an initially abrupt compositional discontinuity at the boundary between the two growth stages that was subsequently modified by intracrystalline diffusion acting to reduce the steep gradient. The position of the boundary with respect to the zoning anomaly is consistent with post-hiatus garnet growth at different P–T conditions or changed garnet-forming reaction.

The varied compositional patterns recorded in different porphyroblasts analysed in this study emphasise the findings of Stallard (1998) that P–T–t estimates can be difficult in polydeformed rocks in which the timing of porphyroblasts growth is uncertain and different porphyroblasts preserve contrasting growth histories, composition and microstructures.

6.3. Controls on porphyroblast growth

The zoning patterns and structural data presented in this study suggest a pause in garnet growth between the proposed G_1 and G_2 growth stages, and contrasting growth histories between different porphyroblasts (e.g. compare BV9 030L and BV5 120 in Table 1). If porphyroblast growth is episodic and temporally variable, then what are

Table 3
Comparison of microstructural and chemical changes across the G_1 boundary and across the boundary between the G_2 and G_3 growth stages

	Microstructures	Inclusion mineralogy	Compositional anomalies	Scale and significance of hiatus	Published examples
Changes across boundary between G_1 and subsequent growth stages	Abrupt truncations	Abrupt changes	Pronounced spikes, reversals and steepened gradients	Regional, inter-orogenic?	Rumble and Finnerty (1974); Karabinos (1984)
Changes across G_2–G_3 boundary	Truncated in places, smoothly curving across boundary in places	No change	Subtle reversals or no change	Local, intra-orogenic?	Spiess and Bell (1996)

the controls on porphyroblast growth during orogenisis? The traditional and widely accepted view is that *P*–*T*-fluid conditions and reaction history are the dominant controls on porphyroblast growth. Recent studies have also emphasised a fundamental linkage between matrix microstructures and porphyroblast growth (Bell et al., 1986; Jones, 1994; Williams, 1994; Spiess and Bell, 1996). Deformational micro-environments such as fold hinges may be favourable sites for porphyroblast nucleation and growth (e.g. Williams, 1994) and there is also evidence for the role of a developing cleavage in controlling the timing of porphyroblast growth. Spiess and Bell (1996) proposed that porphyroblast growth may cease due to the termination of micrometasomatic access of material to the porphyroblast margins as the adjacent matrix foliation intensifies against the porphyroblast edge. The growth patterns indicated in Table 1 suggest that factors in addition to *P*–*T* conditions affected garnet growth in the Fleur de Lys Supergroup, because porphyroblasts from adjacent outcrops have different growth histories. The strong link between poprhyroblast growth, foliation development, and folding in the Fleur de Lys Supergroup (Fig. 1; Stallard, 1998) suggests microstructural, as well as metamorphic controls influenced porphyroblast nucleation and growth.

6.4. Tectonic context

A hiatus in mineral growth, such as that interpreted between the G_1 and G_2 stages of garnet growth, may represent anything from a relatively brief hiatus within a continuous deformation event to a protracted hiatus separating distinct deformation events of contrasting kinematic and metamorphic character. Karabinos (1984) identified two stages of garnet growth from studies in southeast Vermont, and speculated that the garnet cores may be Taconic and the rims Acadian, or alternatively that both the cores and rims are Acadian in age. Rumble and Finnerty (1974) distinguished cores and rims in garnet from eastern Vermont based upon petrographic and compositional criteria and suggested that the cores grew during Ordovician contact metamorphism, whereas the rim overgrowths formed during Devonian regional metamorphism.

In this study, the G_1–G_2 boundary may represent an extended hiatus within a continuous orogenic cycle, as depicted in Fig. 7, or it may indicate a pause in growth between distinct orogenic events of fundamentally different kinematic and metamorphic conditions. By contrast, the G_2–G_3 boundary, if marked by a hiatus, may represent a pause in growth during a continuous orogenic event, marking the transition between successive crenulation cleavages, without change in *P*–*T* conditions, garnet-forming reaction or included mineral phases (Table 3).

In the context of the Newfoundland Appalachian Orogen, the foliations S_3 to S_6 (and G_2, G_3 and G_4) are interpreted to represent a repeated cycle of foliation development and associated garnet growth during the main phase of orogenesis equating with the Salinic Orogeny as described by Cawood et al. (1995), while S_1 and S_2 (and G_1) probably occured early within this event (as shown in Fig. 7) or within the earlier Taconian II metamorphism as described by Cawood et al. (1995). Absolute dating may be the only method of assessing the temporal extent of the hiatus in garnet growth at the G_1–G_2 boundary.

7. Conclusions

Garnet porphyroblasts in the Fleur de Lys Supergroup contain pronounced compositional anomalies coincident with microstructural truncations and changes in inclusion mineral assemblage at the margin of the G_1 stage of garnet growth. The G_1–G_2 boundary is thus interpreted to represent a hiatus in garnet growth, possibly accompanied by garnet consumption. During this pause in growth, changes occurred in the dominant mineral-forming reactions, and *P*–*T* and kinematic conditions, resulting in the observed compositional anomalies and microstructural truncations at the G_1 margin. By contrast, the G_2–G_3 boundary is marked by subtle zoning anomalies, and locally by uninterrupted zoning, suggesting garnet growth may have been continuous across this boundary.

Of the porphyroblasts analysed in this study, those with contrasting microstructural and growth histories also contain contrasting zoning profiles. This supports the previous recognition of contrasting growth histories between individual porphyroblasts from the same outcrop.

Acknowledgements

We thank Michael Williams and Michael Jercinovic of the University of Massachusetts for microprobe analyses (colour maps) used in this study. Various versions of this manuscript have been improved by helpful criticism from Tim Bell, Mike Rubenach, Mike Williams, Bob Tracey, Roger Gibson, Andy Barker, Dyk Eusden, Helen Lang and Peter Hudleston. Annabel Boyes is thanked for her assistance in the field. Generous Newfoundland hospitality provided by E. and C. Traverse of Baie Verte is gratefully acknowledged. The senior author conducted this research with the financial aid of a James Cook University Merit Research Award, and a JSPS Fellowship at Shizuoka University, Japan, during the latter stages of manuscript preparation.

References

Aerden, D.G.A.M., 1995. Porphyroblast non-rotation during crustal extension in the Variscan Lys–Caillaouas Massif, Pyrenees. Journal of Structural Geology 17, 709–725.

Bell, T.H., Fleming, P.D., Rubenach, M.J., 1986. Porphyroblast nucleation, growth and dissolution in regional metamorphic rocks as a function of deformation partitioning during foliation development. Journal of Metamorphic Geology 4, 37–67.

Blackburn, W.H., Navarro, E., 1977. Garnet zoning and polymetamorphism in the eclogitic rocks of Isla de Margarita, Venezuela. Canadian Mineralogist 15, 257–266.

Brown, T.H., Berman, R.G., Perkins, E.H., 1988. Ge0-CALC: Software package for calculation and display of pressure–temperature-composition phase diagrams using an IBM or compatible personal computer. Computers and Geosciences 14, 279–289.

Carlson, W.D., 1989. The significance of intergranular diffusion to the mechanisms and kinetics of porphyroblast crystallization. Contributions to Mineralogy and Petrology 103, 1–24.

Cawood, P.A., Dunning, G.R., Lux, D., van Gool, J.A.M., 1994. Timing of peak metamorphism and deformation along the Appalachian margin of Laurentia in Newfoundland: Silurian, not Ordovician. Geology 22, 399–402.

Cawood, P.A., van Gool, J.A.M., Dunning, G.R., 1995. Collisional tectonics along the Laurentian margin of the Newfoundland Appalachians. In: Hibbard, J.P., van Staal, C.R., Cawood, P.A. (Eds.). Current Perspectives in the Appalachian–Caledonian Orogen. Geological Association of Canada, pp. 283–301 Special Paper 41.

Chernoff, C.B., Carlson, W.D., 1997. Disequilibrium for Ca during growth of pelitic garnet. Journal of Metamorphic Geology 15, 421–438.

Cygan, R.T., Lasaga, A.C., 1982. Crystal growth and the formation of chemical zoning in garnets. Contributions to Mineralogy and Petrology 79, 187–200.

Daniel, C.G., Spear, F.S., 1998. Three-dimensional patterns of garnet nucleation and growth. Geology 26, 503–506.

Davis, B.K., 1995. Regional-scale foliation reactivation and re-use during formation of a macroscopic fold in the Robertson River Metamorphics, north Queensland, Australia. Tectonophysics 242, 293–311.

Erambert, M., Austrheim, H., 1993. The effect of fluid and deformation on zoning and inclusion patterns in poly-metamorphic garnets. Contributions to Mineralogy and Petrology 115, 204–214.

Florence, F.P., Spear, F.S., 1993. Influences of reaction history and chemical diffusion on P–T calculations for staurolite schists from the Littleton Formation, northwestern New Hampshire. American Mineralogist 78, 345–359.

Grover, T.W., Rice, J.M., Carey, J.M., 1992. Petrology of aluminous schist in the Boehls Butte region of northern Idaho: phase equilibria and P–T evolution. American Journal of Science 292, 474–507.

Hames, W.E., Menard, T., 1993. Fluid-assisted modification of garnet composition along rims, cracks, and mineral inclusion boundaries in samples of amphibolite facies schists. American Mineralogist 78, 338–344.

Hibbard, J., 1983. Geology of the Baie Verte Peninsula, Newfoundland. Newfoundland Department of Mines and Energy, Mineral Development Division, Memoir 2, 279pp.

Hickmott, D., Spear, F.S., 1992. Major- and trace-element zoning in garnets from calcareous pelites in the NW Shelburne Falls Quadrangle, Massachusetts: garnet growth histories in retrograded rocks. Journal of Petrology 33, 965–1005.

Ikeda, T., 1993. Compositional zoning patterns of garnet during prograde metamorphism from the Yanai district, Ryoke metamorphic belt, southwest Japan. Lithos 30, 109–121.

Irwin, J.J., 1994. A laser microprobe, mass spectrometric study of Ar, Kr, K, Cl and Br in an "unconformity garnet", associated fluid inclusions, staurolite and micas from Vermont, USA. Chemical Geology 115, 153–170.

Jamieson, R.A., 1990. Metamorphism of an Early Palaeozoic continental margin, western Baie Verte Peninsula, Newfoundland. Journal of Metamorphic Geology 8, 269–288.

Jamieson, R.A., Vernon, R.H., 1987. Timing of porphyroblast growth in the Fleur de Lys Supergroup, Newfoundland. Journal of Metamorphic Geology 5, 273–288.

Jamieson, R.A., O'Beirne-Ryan, A.M., 1991. Decompression-induced growth of albite porphyroblasts, Fleur de Lys Supergroup, western Newfoundland. Journal of Metamorphic Geology 9, 433–439.

Johnson, S.E., 1992. Sequential porphyroblast growth during progressive deformation and low-P high-T metamorphism, Cooma Complex, Australia: the use of microstructural analysis to better understand deformation and metamorphic histories. Tectonophysics 214, 311–339.

Jones, K.A., 1994. Progressive metamorphism in a crustal-scale shear zone: an example from the Leon region, north-west Brittany, France. Journal of Metamorphic Geology 12, 69–88.

Karabinos, P., 1984. Polymetamorphic garnet zoning from southeastern Vermont. American Journal of Science 284, 1008–1025.

Lang, H.M., 1996. Pressure–temperature-reaction history of metapelitic rocks from the Maryland Piedmont on the basis of correlated garnet zoning and plagioclase-inclusion composition. American Mineralogist 81, 1460–1475.

Reeder, J.R., Fagioli, R.O., Meyers, W.J., 1990. Oscillatory zoning of Mn in solution-grown calcite crystals. Earth-Science Reviews 29, 39–46.

Rumble, D., Finnerty, T.A., 1974. Devonian grossularite–spessartine overgrowths on Ordovician almandine from eastern Vermont. American Mineralogist 59, 558–562.

Spear, F.S., 1993. Metamorphic phase equilibria and pressure–temperature–time paths. Mineralogical Society of America Monograph, 799pp.

Spiess, R., Bell, T.H., 1996. Microstructural controls on sites of metamorphic reaction: a case study of the interplay between deformation and metamorphism. European Journal of Mineralogy 8, 165–186.

Stallard, A.R., 1998. Episodic porphyroblast growth in the Fleur de Lys Supergroup, Newfoundland: timing relative to the sequential development of multiple crenulation cleavages. Journal of Metamorphic Geology 16, 711–728.

Williams, M.L., 1994. Sigmoidal inclusion trails, punctuated fabric development, and interactions between metamorphism and derformation. Journal of Metamorphic Geology 12, 1–21.

Young, E.D., Rumble, D., 1993. The origin of correlated variations in in-situ $^{18}O/^{16}O$ and elemental concentrations in metamorphic garnet from southeastern Vermont, USA. Geochemica et Cosmochimica Acta 57, 2585–2597.